Estuaries and Coasts (2014) 37:847–863
DOI 10.1007/s12237-013-9737-6

The Influence of Coastal Nutrients on Phytoplankton Productivity in a Shallow Low Inflow Estuary, Drakes Estero, California (USA)

Christina M. Buck · Frances P. Wilkerson · Alexander E. Parker · Richard C. Dugdale

Received: 17 May 2013 / Revised: 11 October 2013 / Accepted: 21 October 2013 / Published online: 24 December 2013

Abstract Seasonal wind-driven upwelling along the U.S. West Coast supplies large concentrations of nitrogen to surface waters that drives high primary production. However, the influence of coastal upwelled nutrients on phytoplankton productivity in adjacent small estuaries and bays is poorly understood. This study was conducted in Drakes Estero, California, a low inflow estuary located in the Point Reyes National Seashore and the site of an oyster mariculture facility that produces 40 % of the oysters harvested in California. Measurements of nutrients, chlorophyll *a*, phytoplankton functional groups, and phytoplankton carbon and nitrogen uptake were made between May 2010 and June 2011. A sea-to-land gradient in nutrient concentrations was observed with elevated nitrate at the coast and higher ammonium at the landward region. Larger phytoplankton cells (>5 μm diameter) were dominant within the outer and middle Estero where phytoplankton primary productivity was fueled by nitrate and *f*-ratios were >0.5; the greatest primary production rates were in the middle Estero. Primary production was lowest within the inner Estero, where smaller phytoplankton cells (<5 μm) were dominant, and nitrogen uptake was dominated by ammonium. Phytoplankton blooms occurred at the outer and middle Estero and were dominated by diatoms during the spring and dry-upwelling seasons but dinoflagellates during the fall. Small flagellated algae (>2 μm) were dominant at the inner Estero where no blooms occurred. These results indicate that coastal nitrate and phytoplankton are imported into Drakes Estero and lead to periods of high new production that can support the oyster mariculture; a likely scenario also for other small estuaries and bays.

Keywords Coastal nutrients · Phytoplankton productivity · Drakes Estero · California · Low inflow estuary

Communicated by James L Pinckney

C. M. Buck · F. P. Wilkerson (✉) · A. E. Parker · R. C. Dugdale
Romberg Tiburon Center for Environmental Studies, San Francisco State University, 3152 Paradise Drive, Tiburon, CA 94920, USA
e-mail: fwilkers@sfsu.edu

Present Address:
A. E. Parker
California Maritime Academy, 200 Maritime Academy Drive, Vallejo, CA 94590, USA

Introduction

Bivalve shellfish aquaculture, particularly for *Crassostrea gigas* (Pacific oyster) and *Ruditapes philippinarium* (Manila clam), is well established in estuaries along the U.S. West Coast (e.g., Willapa Bay, Washington; Coos Bay, Oregon; Tomales Bay, California). This is considered to be due in part to high primary production fueled by coastal upwelled nutrients as described for the Washington and Oregon estuaries (Dumbauld et al. 2009). Recently there has been interest in how ocean-derived nutrients help to fuel primary and secondary estuarine production, including mariculture facilities within temperate regions (Roegner et al. 2002; Ruesink et al. 2003; Kimbro et al. 2009). At present, detailed studies have been carried out primarily in U.S. East Coast estuaries (e.g., Neuse River Estuary) and in the dominant estuaries on the U.S. West Coast (e.g., the San Francisco Estuary) but relatively little is understood about the dynamics of nutrient supply, dominant phytoplankton groups, and primary production in the many smaller estuaries that exist along the U.S. West Coast. There are few measurements of primary production and none of phytoplankton nutrient uptake.

Most estuaries along California, Oregon, and Washington lie adjacent to upwelling centers, where cold, salty, nutrient-rich waters are brought to the ocean surface during prolonged equatorward winds. Similar situations occur in other eastern boundary systems such as Baja California (Mexico), South

Africa, Spain, and Western Australia (Largier 2010). Mesotidal conditions (Hickey and Banas 2003) combined with small estuary size can contribute to substantial tidal exchange with the ocean (Dumbauld et al. 2009) and the import of nutrient rich water into these estuaries (e.g., Hickey 1989; Monteiro et al. 1998; Hickey and Banas 2003; Ruesink et al. 2003) such that upwelled water may be the predominant nutrient source seasonally for primary production (e.g., in Yaquina Bay, OR; Willapa Bay, WA; and Saldahna Bay, South Africa; Newton and Horner 2003; Banas et al. 2007; Brown and Ozretich 2009; Monteiro et. al. 1998).

Along upwelling coasts within mid latitudes there are small shallow estuaries with small watersheds that have been classified as low inflow estuaries (LIEs) (Largier 2010). These estuaries, with a Mediterranean climate, experience extended dry seasons with low freshwater inflow (Largier 2010; Largier et al. 1997). During the dry season the input of terrestrial nutrients is minimized due to low precipitation and runoff. During the dry season in LIEs, the input of freshwater from riverine sources may be less than evaporative losses, resulting in long water residence time and hypersalinity in the upper reaches (Largier 2010). However this occurs at the same time as elevated coastal upwelling in eastern boundary systems including central California (Kimbro et al. 2009; Largier 2010) such that nutrients may be supplied from an ocean source.

LIEs are ecologically important. For example, in California the three major shellfish growing areas (Humboldt Bay, Tomales Bay, and Drakes Estero) (Dumbauld et al. 2009) are all LIEs (Largier 2010) as is the maricuture region in Bahía San Quintin, Mexico (Montes-Hugo 2007). Poorly studied (Largier 2010) but have exhibited interesting patterns. Kimbro et al. (2009) observed elevated chlorophyll *a* due to coastally derived nutrients in the middle of Tomales Bay, California, resulting in higher growth rates of the native Olympia oyster (*Ostreola conchapilia*). Patterns of nutrient concentrations are variable with season and due to surrounding watershed input. In the more pristine estuaries the low mixing and hypersalinity in the inner reaches of LIEs may lead to depletion or build up of nutrients. Smith and Hollibaugh (1997) described increased phosphate and lower DIN concentrations within the inner hypersaline reaches of the Tomales Bay, CA.

Drakes Estero, California, is a low inflow estuary located within the Point Reyes National Seashore, California (Fig. 1), and lies adjacent to Drakes Bay, the site of an upwelling shadow where there is an enhanced positive relationship between upwelling intensity and primary production (Largier 2004; Vander Woude et al. 2006). Drakes Estero was designated as potential wilderness area in 1976 and as a California State Marine Conservation Area in 2010. Land use surrounding the Estero includes historic cattle farming while the Estero itself has been used for oyster mariculture since the 1930s. The removal of the oyster mariculture has been mandated to meet the wilderness designation (U.S. Department of the Interior 2012). There are few published studies that describe the ecology of the Estero and there are no studies that describe baseline seasonal data of nutrients, phytoplankton biomass, primary production or nutrient uptake, or that indicate how these may change with oyster removal.

The use of different chemical forms of nutrients, specifically dissolved inorganic nitrogen (DIN), for phytoplankton productivity to supply upper trophic levels and fisheries yield (including mariculture) has been considered using the concepts of "new" and "regenerated" production, first introduced by Dugdale and Goering (1967), using the stable isotope ^{15}N as a tracer to track phytoplankton uptake of nitrate (NO_3) and ammonium (NH_4). They showed that in the ocean, NO_3 uptake can provide a proxy for new production that is directly related to yield, and NH_4 a proxy for regenerated production. In estuaries, defining new and regenerated production is challenging because several forms of nitrogen (N) (e.g., NO_3, NH_4, and urea) may be supplied by river runoff and anthropogenic sources, and represent "new" N. During the dry-upwelling season, elevated NO_3 input into LIEs should support new production from coastally upwelled sources, since land based runoff is minimized, although this has not been tested using $^{15}NO_3$ uptake by LIE phytoplankton.

In addition to the influence on phytoplankton productivity, the chemical form of N supplied, as well as seasonal conditions, will influence the functional groups that dominate the phytoplankton community. The classic observations of Margalef (1978) indicate temperate phytoplankton blooms to be diatom-dominated in the spring when NO_3 is abundant and dinoflagellate-dominated in the fall. More recently, in the Rias Baixas of Galicia, an upwelling region of Spain, Figueiras et al. (2002) observed diatoms during the upwelling season when there was wind driven upwelling and NO_3 was the dominant form of DIN, while dinoflagellates dominated during relaxation events when NH_4 was the major form of DIN. Along the U.S. West Coast, Dugdale et al. (2006) reported more new production, higher phytoplankton yield, and diatoms to result from elevated NO_3 supply during upwelling. How the phytoplankton functional groups may change in the Estero with different nutrient conditions is unclear.

The purpose of this study was to investigate the seasonal and spatial patterns of phytoplankton response to different seasonal nutrient regimes in Drakes Estero and provides the first ^{15}N tracer nutrient uptake rates for a LIE adjacent to an upwelling center on the U.S. West Coast. We expected that seasonal shifts in nutrient sources due to the Mediterranean climate and proximity to an upwelling region would drive seasonal variation in quantity and location of primary production and phytoplankton N use, along with changes in

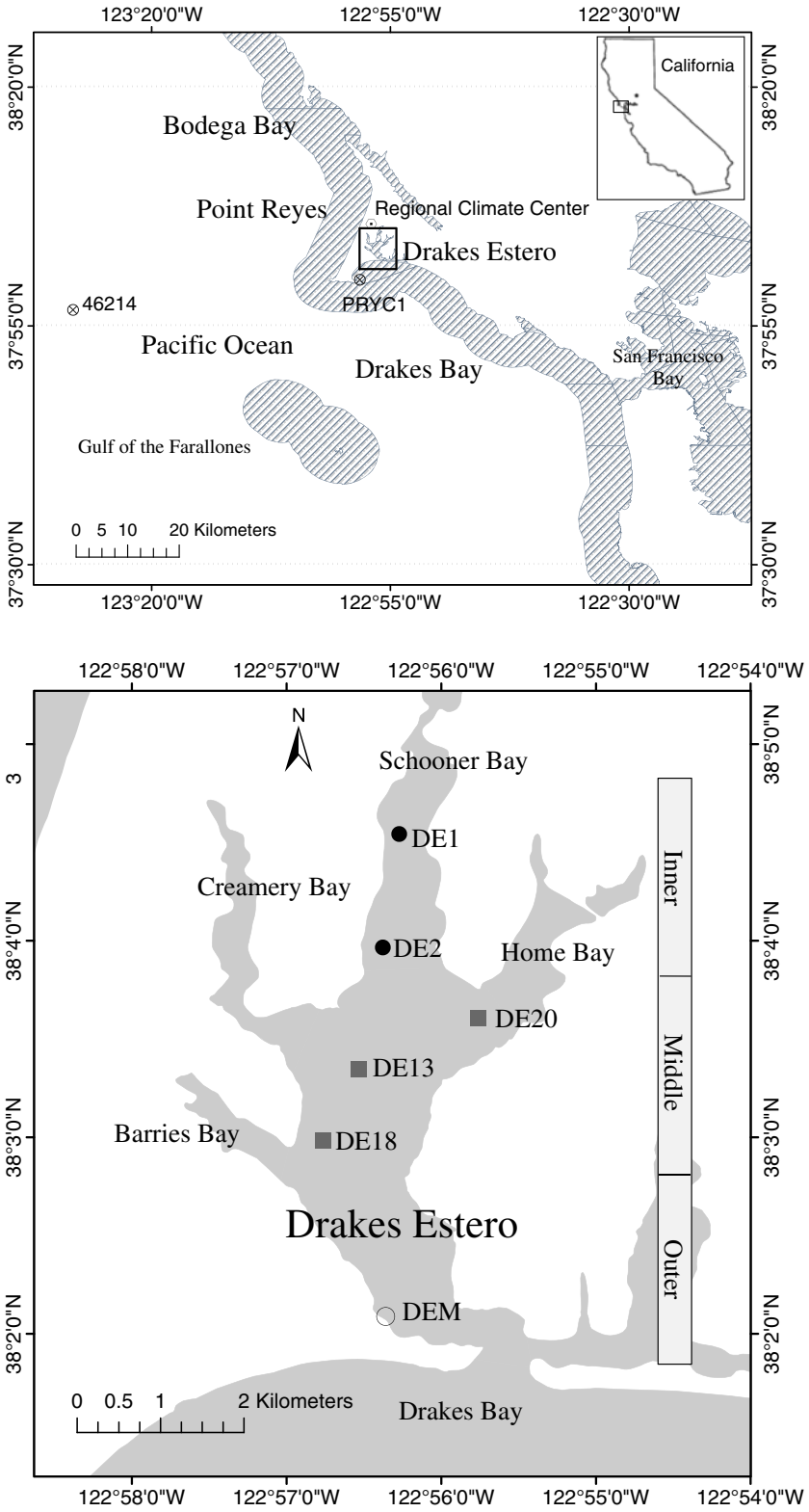

Fig. 1 Map of study area and Drakes Estero, California. The inner Estero sites (DE1, DE2) are represented by closed circles, middle Estero sites (DE20, DE18, DE13) are represented by *grey squares*, and outer site (DEM) is represented by *open circles*

dominant phytoplankton functional groups. In this LIE, coastally derived NO_3 will likely drive primary production (new production) at the outer Estero and lead to diatom abundance, while at the inner reaches of the Estero (regenerated and external land based production) will likely be fueled by NH_4 and result in fewer diatoms.

Methods

Study Site

Drakes Estero is located on the south coast of the Point Reyes Peninsula, California (Fig. 1) with a Mediterranean climate having distinct wet (November to May) and dry (June to October) seasons (Largier et al. 1997). The total Estero area is 9.4 km^2 at high tide with approximately half of the area, 4.8 km^2 exposed at low tide. Mean water depth is <2 m except for an 8-m-deep channel that runs through the main axis of the Estero. The semidiurnal tidal range is approximately 2 m, and all tidal exchange occurs through one narrow opening connected to Drakes Bay (Fig. 1). Freshwater input is from six perennial streams and four ephemeral streams with an 80 km^2 watershed.

Regional Setting

Regional environmental data were downloaded from databases administered by the Western Regional Climate Center (WRCC) or the National Ocean and Atmospheric Administration (NOAA). Precipitation was acquired from the WRCC daily time series database for the Point Reyes Riparian Conservation Area (RCA) station located 2 km northwest of Drakes Estero (location 38°5.64′N, 122°57.0′W; www.wrcc.dri.edu/weather/prca.html). Regionally calculated daily Bakun upwelling index values from May 2010 to June 2011were acquired for the Pacific region 36°N 122°W from the database maintained by NOAA Pacific Fisheries Environmental Laboratory. (http://www.pfeg.noaa.gov/products/pfel/modeled/indices/upwelling/NA/data_download.html). Sea surface temperatures were obtained from NOAA's National Bouy Center historical databases for the offshore Pacific Ocean buoy at station 46214 (location 37°56.7′N, 123°28.2′W; http://www.ndbc.noaa.gov/station_page.php?station=46214); and for Drakes Bay at the Point Reyes, California station (PRYC1) (location 37°59.820′N, 122°58.800′W; http://www.ndbc.noaa.gov/station_page.php?station=pryc1).

Field Sampling

The Estero was sampled biweekly except for December, January, and February, when it was sampled monthly, from May 2010 to June 2011 for a total of 23 dates. Seasonal classifications were defined as the dry-upwelling season between 10 June to 15 October 2010; the winter season from 3 November 2010 to 3 March 2011; and the spring transitional seasons as 28 May to 9 June 2010 and 3 March to 16 June 2011 and the fall transitional period as 16 October to 22 November 2010. The Estero was divided into three regions (Fig. 1), inner (stations DE1, DE2), middle (stations DE13, DE18, DE20), and the outer (site DEM) regions. The inner and middle regions site selection was based on previously established water quality sampling stations (California Department of Public Health 2010) and DEM (38°02.095′N; 122°56.359′W) was selected as an outer site due to accessibility from land by wading. Sample collection was by small boat at all sites except for DEM. On 16 April 2010, 14 July 2010, and 1 June 2011 surface samples were collected from DEM hourly for 9, 13, and 12 h, respectively, to measure variables over the tidal cycle.

Surface temperature and salinity were measured using an YSI 85 probe. Salinity is reported using the practical salinity scale. Water clarity was not measured directly. However a Secchi disk was deployed at every sampling and was always visible to the bottom (except at DE1 on 3 March 2011). Surface water samples were collected for analysis of nutrients, chlorophyll *a*, phytoplankton enumeration, and carbon and nitrogen uptake rates using 500-ml amber polycarbonate bottles, then stored on ice and transported by car within 6 h for processing to the Romberg Tiburon Center for Environmental Studies, Tiburon, CA.

Analytical Methods and Calculations

All samples collected for nutrient analysis were filtered through Whatman GF/F filters. A Bran and Luebbe AutoAnalyzer II with MT-19 manifold chemistry module was used for NO_3+nitrite (NO_2) and NO_2 analysis according to Whitledge et al. (1981) and Bran and Luebbe Inc. (1999c) Method G-172-96, phosphate (PO_4) according to Bran and Luebbe Inc. (1999b) Method G-175-96 and silicate ($Si(OH)_4$) by Bran and Luebbe Inc. (1999a) Method G-177-96 and MacDonald et al. (1986). NO_3+NO_2 is referred to as NO_3 throughout the text as NO_2 concentrations measured were<1.0 μmol l^{-1}. Ammonium concentrations were determined using the colorimetric method of Solorzano (1969). Urea was analyzed using the method of Revilla et al. (2005). Both NH_4 and urea analyses were made using a Hewlett Packard diode array spectrophotometer and 10-cm path length cell. DIN was calculated as the sum of NO_3+NO_2 plus NH_4 concentrations.

Water samples (50–100 ml) to be analyzed for chlorophyll *a* were filtered under a low vacuum <250 mmHg); for total chlorophyll *a* (chl *a*) on Whatman GF/F filters (nominal pore size 0.7 μm) and for size fractionated chlorophyll *a* (i.e., chl *a* in cells >5 μm) on 5-μm pore-sized Nuclepore polycarbonate filters. The filters were stored dry in glass culture tubes in the dark at −80 °C and analyzed for chlorophyll *a* within 2 weeks of sampling. Chlorophyll *a* was extracted from the filters in 90 % acetone for 24 h at 4 °C according to Arar and Collins (1992). Analysis was performed fluorometrically with a Turner Designs™ Model 10-AU using 10 % hydrochloric acid to correct for and measure phaeophytin. The fluorometer was calibrated with Turners Designs™ chlorophyll *a*

standard. Phytoplankton blooms were defined as chl *a* concentrations >8 μg l^{-1}.

Phytoplankton carbon and nitrogen uptake was measured using tracer additions (~10 % of ambient concentration) of ^{15}N labeled NH_4, $^{15}NO_3$ and ^{13}C labeled bicarbonate (using ^{15}N or ^{13}C at 99 at.%). Two 160-ml clear polycarbonate incubation bottles were filled with surface water at each station; to one incubation bottle $NaH^{13}CO_3$ and $^{15}NH_4Cl$ were added and to the other, $NaH^{13}CO_3$ and $K^{15}NO_3$ Samples were incubated under window screening at 50 % of surface light for 24 h in an incubation table cooled with San Francisco Central Bay water with observed ambient seasonal mean temperature between 11.5 ° and 17.4 ° C (Wilkerson et al. 2006a). During the 24-h sampling period, the San Francisco Central Bay temperatures were within 6 °C of the ambient temperatures from when the samples were collected in Drakes Estero, and showed the same seasonal trends as the Drakes Estero values. We did not attempt to account for NH_4 regeneration and reported NH_4 uptake rates should be considered conservative. Incubations were terminated by gentle vacuum filtration onto pre-combusted (450 °C for 4 h) 25-mm diameter Whatman GF/F filters and frozen until analysis. Phytoplankton ^{13}C and ^{15}N enrichment as well as concentrations of particulate carbon (POC) and nitrogen (PON) were measured on a Europa PDZ 20/20 gas chromatograph-mass spectrometer. Nitrogen and carbon uptake rates (ρ, μmol l^{-1} day^{-1}) and biomass-specific uptake (normalized to either POC or PON, *V*, day^{-1}) were calculated according to Dugdale and Wilkerson (1986) and Legendre and Gosselin (1996). Assimilation numbers were calculated by normalizing ρC to chlorophyll *a*. Phytoplankton carbon uptake rates (ρC) are referred to as "primary production" as is the convention for carbon uptake studies.

The f-ratio describes the fraction of nitrogen uptake that is in the form of NO_3 and was calculated by dividing the sum of ρNO_3 and ρNH_4 by ρNO_3 (Dugdale and Goering 1967). An estimate of depth-integrated C uptake (mg C m^{-2} day^{-1}) for the water column was calculated by multiplying ρC and by high tide depth assuming that phytoplankton were light-saturated throughout the water column. Annual integrated estimates of primary production were calculated for DE18 (depth 3 m) and DE1 (depth 1.5 m).

Water samples (250 ml) for phytoplankton enumeration were collected on 8 July 2010, 4 November 2010 and 10 May 2010 at each station and preserved with Lugol's solution. These dates corresponded to periods of elevated phytoplankton biomass as determined by chlorophyll *a*. Samples were kept in the dark at room temperature until they were counted. Phytoplankton were enumerated by microscopic identification using the Utermöhl inverted microscope technique (Lund et al. 1958). Aliquots of 27 ml Lugols preserved sample were settled for a minimum of 18 h and counted at 400× magnification with a Nikon Diaphot Phase Contrast inverted microscope. Phytoplankton were identified and placed in the following functional groups: centric diatoms, pennate diatoms, dinoflagellates, eukaryotic flagellate algae (2–200 μm), and other (nonclassified functional group). Picoeukaryotic phytoplankton were not counted.

Spatial and temporal patterns in the data were investigated using one-way ANOVA; *p* and *F* values and degrees of freedoms are provided.

Results

Regional Setting

The dry-upwelling season occurred between 10 June to 15 October 2010 when there was 0.2 cm rainfall and high positive offshore Bakun upwelling indices (Fig. 2). Upwelling indices are a calculated value based on estimates of offshore Ekman transport driven by geostrophic wind stress and positive values indicate equatorward wind stress — the condition for coastal upwelling (Bakun 1973). The winter season (23 November 2010 to 3 March 2011) had higher precipitation and generally negative Bakun upwelling indices (non- upwelling conditions, Bakun 1973) (Fig. 2). The spring and fall transitional periods (28 May to 10 June 2010 and 3 March to 16 June 2011; 16 October to 22 November 2010) were both characterized by measureable precipitation and elevated upwelling in spring, but minimal upwelling in the fall. During May and June 2011 there were unseasonably large storms that resulted in nearly 7.5-fold higher precipitation compared to the same period in 2010 (Fig. 2a).

The offshore sea surface temperature (SST) in the Pacific Ocean was coldest (8–12.5 °C) during the extended periods of upwelling and Drakes Bay SST was generally warmer (10–16 °C) than offshore (Fig. 2c). The SST in Drakes Bay and offshore were similar during the wet seasons, and offshore temperatures were warmest from mid-September to November when the Bakun upwelling index decreased and precipitation increased (Fig. 2c).

Temperature and Salinity in the Estero

Temperatures in the outer and middle Estero (Fig. 3a) were similar to Drakes Bay (Fig. 2c). Water temperatures were significantly higher at the inner Estero (ANOVA, $F(2,131)=17.71$, $p<0.005$) except for winter when temperatures were similar throughout the Estero (ANOVA, $F(2,26)=0.11$, $p=0.90$) and the adjacent coastal ocean (Table 1; Figs. 2c and 3a). The inner Estero exhibited the largest seasonal range in water temperatures, with a minimum of 11.1 °C in the winter and maximum of 19.4 °C in the dry-upwelling season (Fig. 3a).

Salinity varied between 18.9 and 36.2 throughout sites in the Estero, reflecting the low freshwater inflow and oceanic

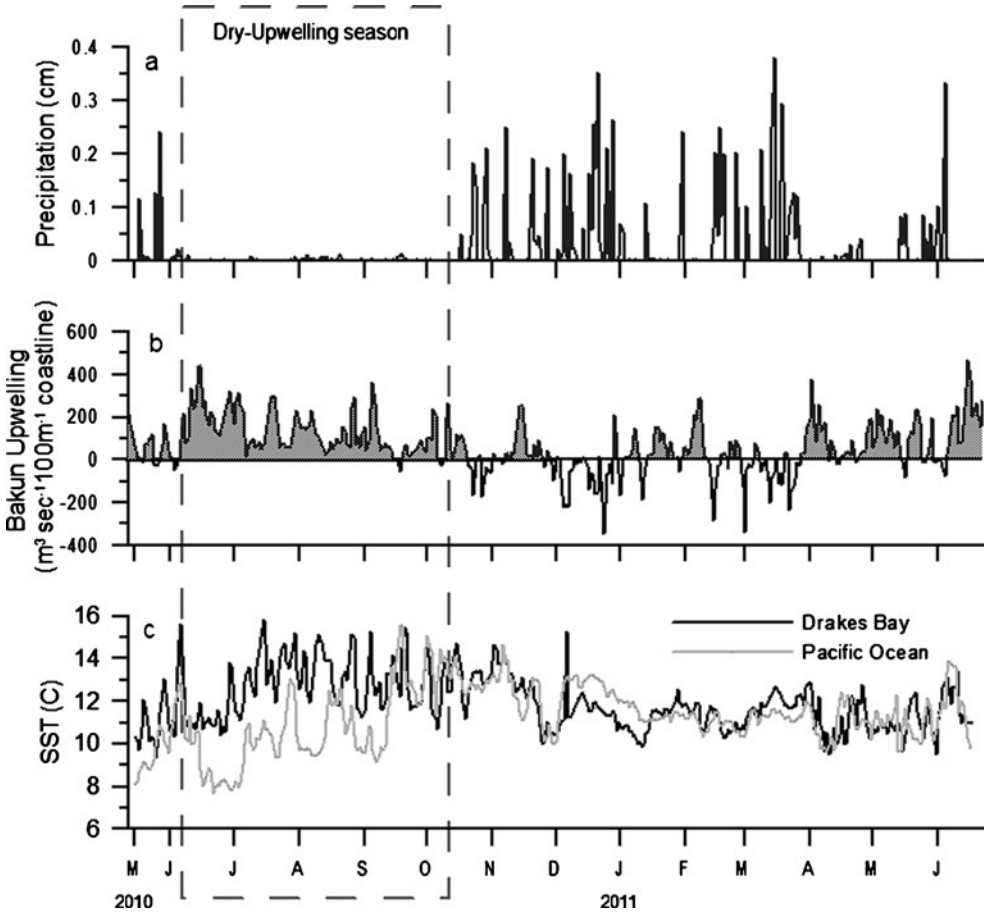

Fig. 2 Regional temporal conditions for Drakes Bay and adjacent Pacific Ocean from May 2010 to June 2011. **a** Total daily precipitation, **b** Bakun upwelling index with positive upwelling shaded in *dark grey*, **c** daily mean sea surface temperature (*SST*) for Drakes Bay (PRYC1 buoy) and offshore Pacific Ocean (46214 buoy). The dry-upwelling season is indicated by the *dashed box*

influence (Table 1, Fig. 3b). Salinity increased from the outer to inner sites during the dry-upwelling season (Table 2, Fig. 3b). This pattern reversed during the wet seasons (Fig. 3b). The greatest annual range in salinity (18.9–39.9) was observed at DE1 (inner Estero) which was brackish after heavy rainfall but displayed a hypersaline maximum during the dry-upwelling season (Fig. 3b).

Nutrient Concentrations

Annual mean NO_3 concentrations were significantly higher at the outer sites compared to inner sites (t-test, $p < 0.005$) and middle sites compared to inner sites (t-test, $p < 0.005$) (Table 1). At the outer Estero NO_3 was >3.8 μmol l^{-1} in all seasons (Fig. 4a) while at the inner Estero NO_3 averaged 0.7 μmol l^{-1} during the dry-upwelling season and transitional months, but increased more than 10-fold during the winter (Fig. 4a). The outer and middle Estero had greater NO_3 during the dry-upwelling season (Fig. 4a) compared to other seasons (Fig. 4a), with a maximal NO_3 of 36.2 μmol l^{-1} at DE18 (Fig. 4a).

Ammonium concentrations were highest at the inner Estero (DE1 and DE2), and 1.5-fold higher than the outer Estero (DEM; Table 1, Fig. 4b). Ammonium was typically less than NO_3 except at DE1 during the dry-upwelling season (Fig. 4b). The highest mean NH_4 concentrations were observed at the inner Estero (DE2; 3.4 μmol l^{-1}; Table 1), and the greatest absolute values were measured at DE1 (8.3 μmol l^{-1}), in samples collected during both during the winter and dry-upwelling seasons (Fig. 4b).

Estero-wide, mean annual urea concentrations were lower than annual averages for either NH_4 or NO_3 (Table 1). The inner Estero had the greatest annual mean urea of 1.6 μmol l^{-1} compared to the middle and outer Estero (~1 μmol l^{-1}; Table 1). During the dry-upwelling season, urea concentrations at DE1 was similar in value to NH_4 but greater than NO_3 (Fig. 4b, c). The highest urea concentration (3.3 μmol l^{-1}) was measured at DE2 (Fig. 4c).

Phosphate and $Si(OH)_4$ concentrations followed similar trends to NO_3 at the outer and middle Estero (Fig. 4) whereas at the inner Estero PO_4 followed the opposite spatial trend of NO_3 (Fig. 4). Phosphate concentrations were highest during the dry-upwelling season throughout the Estero (Fig. 4d), with the highest concentration (6.1 μmol l^{-1}) at DE1 (Fig. 4d). Increased $Si(OH)_4$ concentrations occurred at DE1 during the winter, with elevated $Si(OH)_4$ (139.5 μmol l^{-1}) measured on 3 March 2011 (Fig. 4e) after heavy precipitation (Fig. 2a) and during the time of lowest measured salinity (Fig. 3b). Within

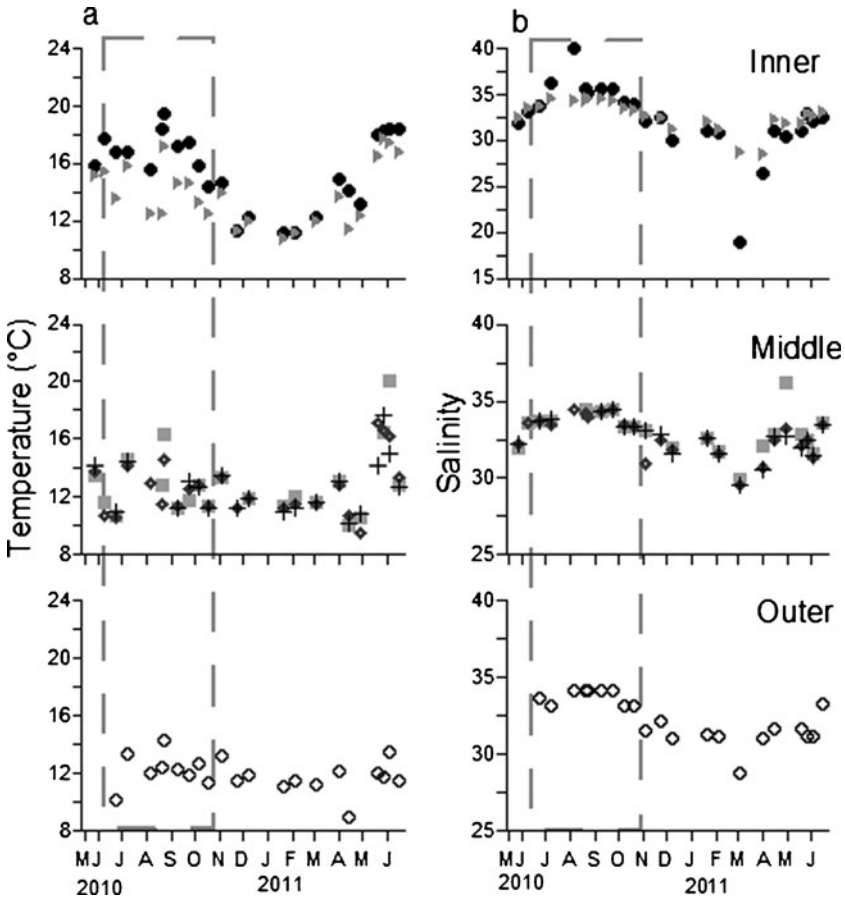

Fig. 3 Time series of **a** temperature and **b** salinity from May 2010 to June 2011. Inner Estero are indicated for DE1 (*filled circle*), DE2 (*filled triangle*); middle sites DE20 (*plus symbol*), DE13 (*empty diamond*), DE18 (*filled square*) and outer site DEM (*empty circle*). The dry-upwelling season is indicated by the *dashed box*

Table 1 Annual mean±(standard deviation) temperature, salinity, nutrients (NO_3, NH_4, urea, PO_4, $Si(OH)_4$), chlorophyll *a* (total and >5-μm size fraction), uptake rates (ρC; ρNO_3, ρNH_4, *V*NO_3 and *V*NH_4), and assimilation number at outer (DEM) to inner Estero locations from May 2010 to June 2011

	Outer Estero		Middle Estero		Inner Estero	
	DEM	DE18	DE13	DE20	DE2	DE1
Temperature (°C)	11.9 (1.2)	12.9 (2.4)	12.7 (2.0)	12.6 (1.8)	13.9 (2.2)	15.5 (2.6)
Salinity	32.3 (1.5)	33.1 (1.3)	32.7 (1.3)	32.6 (1.2)	32.7 (1.6)	32.3 (3.9)
Nitrate (μmol l^{-1})	21.6 (8.6)	18.2 (10.5)	18.1 (10.0)	16.4 (10.4)	7.9 (7.3)	2.4 (3.5)
Ammonium (μmol l^{-1})	2.0 (1.0)	2.0 (0.7)	2.9 (1.5)	2.5 (1.2)	3.4 (1.8)	2.2 (2.2)
Urea (μmol l^{-1})	1.2 (0.6)	1.0 (0.5)	1.3 (0.6)	1.1 (0.5)	1.6 (0.7)	1.6 (0.7)
Phosphate (μmol l^{-1})	2.7 (0.8)	2.6 (0.9)	2.6 (0.9)	2.4 (0.9)	2.6 (0.9)	3.1 (1.4)
Silicate (μmol l^{-1})	36.2 (12.0)	36.1 (13.3)	36.2 (12.2)	34.4 (13.7)	29.5 (11.0)	29.6 (10.2)
Chlorophyll (μg l^{-1})	4.1 (4.3)	2.8 (3.0)	2.6 (2.9)	2.2 (2.2)	1.4 (0.7)	2.0 (1.1)
>5 μm Chl (μg l^{-1})	3.7 (4.3)	2.4 (3.2)	2.2 (2.9)	1.7 (2.2)	0.9 (0.7)	0.9 (0.9)
ρC (μmol l^{-1} day^{-1})	19.18 (27.94)	20.68 (30.62)	13.50 (20.60)	12.95 (15.42)	6.03 (3.88)	6.41 (3.91)
ρNO_3 (μmol l^{-1} day^{-1})	1.05 (1.39)	1.32 (1.20)	1.10 (1.56)	0.71 (0.81)	0.21 (0.17)	0.08 (0.07)
ρNH_4 (μmol l^{-1} day^{-1})	0.98 (0.80)	0.85 (0.75)	0.94 (0.90)	1.02 (1.38)	0.79 (0.87)	0.74 (0.67)
VNO_3 (day^{-1})	0.20 (0.20)	0.27 (0.24)	0.27 (0.48)	0.15 (0.16)	0.06 (0.05)	0.02 (0.02)
VNH_4 (day^{-1})	0.16 (0.08)	0.20 (0.24)	0.24 (0.28)	0.23 (0.22)	0.33 (0.81)	0.17 (0.16)
Assimilation number (mgC mg Chl a^{-1} day^{-1})	55.4 (33.9)	91.5 (64.9)	63.1 (48.0)	76.4 (49.2)	54.1 (24.3)	39.1 (16.3)
f-ratio	0.51 (0.18)	0.53 (0.29)	0.47 (0.25)	0.38 (0.25)	0.27 (0.18)	0.15 (0.14)

Table 2 Dry-upwelling seasonal mean±(standard deviation) temperature, salinity, nutrients (NO_3, NH_4, urea, PO_4, $Si(OH)_4$), chlorophyll *a* (total and >5 μm size fraction), assimilation number, and uptake rates (ρC, ρNO_3, ρNH_4) at outer to inner Estero locations from 10 June to 15 October 2010

	Outer Estero		Middle Estero		Inner Estero	
	DEM	DE18	DE13	DE20	DE2	DE1
Temperature (°C)	12.4 (1.2)	12.9 (2.0)	12.6 (1.4)	12.5 (1.4)	14.3 (1.6)	17.2 (1.3)
Salinity	33.8 (0.5)	34.0 (0.4)	34.0 (0.4)	33.9 (0.5)	34.3 (0.4)	35.7 (1.9)
Nitrate (μmol l^{-1})	25.5 (7.3)	25.3 (10.9)	23.1 (10.0)	23.7 (12.9)	10.7 (7.8)	0.7 (0.9)
Ammonium (μmol l^{-1})	2.0 (1.2)	1.7 (0.6)	2.6 (1.9)	1.6 (0.5)	3.3 (1.4)	2.0 (2.6)
Urea (μmol l^{-1})	1.2 (0.6)	1.2 (0.7)	1.5 (0.8)	1.1 (0.8)	1.6 (0.9)	2.1 (0.4)
Phosphate (μmol l^{-1})	3.2 (0.8)	3.3 (0.9)	3.3 (1.0)	3.3 (1.0)	3.5 (0.7)	4.6 (1.0)
Silicate (μmol l^{-1})	43.1 (10.9)	45.7 (14.5)	43.6 (13.0)	47.5 (15.8)	35.4 (6.9)	36.8 (9.5)
Chlorophyll (μg l^{-1})	4.8 (5.6)	2.4 (2.0)	2.2 (1.7)	2.0 (2.0)	1.2 (0.7)	1.5 (0.6)
>5 μm Chl (μg l^{-1})	4.3 (4.9)	2.0 (1.5)	2.0 (1.8)	1.6 (1.2)	0.8 (0.4)	0.4 (0.21)
ρC (μmol l^{-1} day^{-1})	19.11 (18.41)	21.50 (14.22)	20.98 (28.43)	20.43 (21.18)	8.25 (4.21)	6.62 (2.81)
ρNO_3 (μmol l^{-1} day^{-1})	1.74 (2.22)	1.97 (1.18)	1.29 (1.19)	1.46 (1.08)	0.33 (0.17)	0.07 (0.05)
ρNH_4 (μmol l^{-1} day^{-1})	1.25 (0.40)	1.06 (0.53)	0.93 (0.58)	0.51 (0.21)	0.82 (0.28)	0.73 (0.28)
Assimilation number (mgC mg Chl a^{-1} day^{-1})	64.5 (35.2)	101.0 (17.4)	106.6 (65.7)	104.9 (53.8)	72.9 (20.0)	45.9 (9.2)
f-ratio	0.59 (0.27)	0.64 (0.09)	0.51 (0.20)	0.60 (0.11)	0.31 (0.09)	0.10 (0.08)

the outer and middle Estero, NO_3, PO_4, and $Si(OH)_4$ exhibited similar patterns of change in concentrations between sampling periods (Fig. 4).

DIN to P was less than the Redfield ratio of 16:1 throughout the Estero (Fig. 4f). Because PO_4 was relatively invariant and NH_4 was relatively low, much of the variation in DIN/P was driven by changes in NO_3 concentrations (Fig. 4). The lowest DIN/P (< 2:1) was observed at DE1 (Fig. 4f) when mean NO_3 was <1 μmol l^{-1} (Fig. 4a). DIN/P was ~8:1 during all seasons in the outer Estero, while DIN/P varied between <1:1 to 12:1 in the middle Estero (Fig. 4c).

Chlorophyll *a*

Total chlorophyll *a* concentrations were typically <5 μg l^{-1} and did not exceed 17.6 μg l^{-1} (Fig. 5a). Annual mean chlorophyll *a* decreased from the outer to the inner Estero, with the lowest annual mean observed at DE2 (1.4 μg l^{-1}). No phytoplankton blooms (Fig. 5a) were observed at the inner Estero with an annual average chlorophyll *a* of ≤2 μg l^{-1} (Table 1). DEM had the greatest annual mean chlorophyll *a* (Table 1), with three blooms observed (Fig. 5a) and the highest measured concentration (17.6 μg l^{-1}) on 8 July 2010 (Fig. 5a). The most spatially extensive bloom encompassed the outer and middle Estero during the fall in November 2010 (Fig. 5a). When sampled over tidal cycles chlorophyll *a* concentrations at DEM increased during flood tide, with the maximum chlorophyll *a* observed within an hour of high water (Fig. 6). Chlorophyll *a* varied up to 3-fold from (~0.5 to 3.5 μg l^{-1}) between ebb and flood tides in April and July 2010 (Fig. 6).

Like total chlorophyll *a*, there was a decreasing trend of chlorophyll *a* in >5-μm cells from the outer to inner Estero (Table 1, Fig. 5). The regression slope for the >5-μm chlorophyll *a* versus total chlorophyll *a* was almost 1:1 suggesting a large proportion of the chlorophyll *a* in the outer and middle Estero was contributed by phytoplankton cells >5 μm in diameter (Fig. 7). When plotted only for DE1, the regression slope for the >5-μm chlorophyll *a* versus total chlorophyll *a* was less than 1:1, indicating that >5-μm cells contributed less to total chlorophyll *a*, slightly more than 50 % contribution (Fig. 7).

Carbon Uptake and Assimilation Number

Carbon uptake rates (ρC) were greater at the outer and middle Estero compared to the inner Estero, but not significantly different when a one-way ANOVA was applied (ANOVA, $F(2,100)=2.97$, $p=0.056$) (Table 1, Fig. 5d). Nitrogen uptake rates (ρN) were significantly greater at the outer and middle Estero compared to the inner Estero (ANOVA, $F(2,123)=6.46$, $p=0.002$).

Three peaks in ρC were observed in the middle Estero, one in the dry-upwelling season (8 July 2010), one in the fall transitional season (4 November 2010), and one in the spring transitional season (19 May 2011) (Fig. 5d). These peaks corresponded with phytoplankton blooms observed as chlorophyll *a* (Fig. 5a). The increase in ρC in July 2010 occurred with a large increase in ρNO_3, while the October ρC peak was accompanied by a smaller increase in ρNO_3, and the peak in May 2011 with an slight increase in both ρNO_3 and ρNH_4 (Fig. 5).

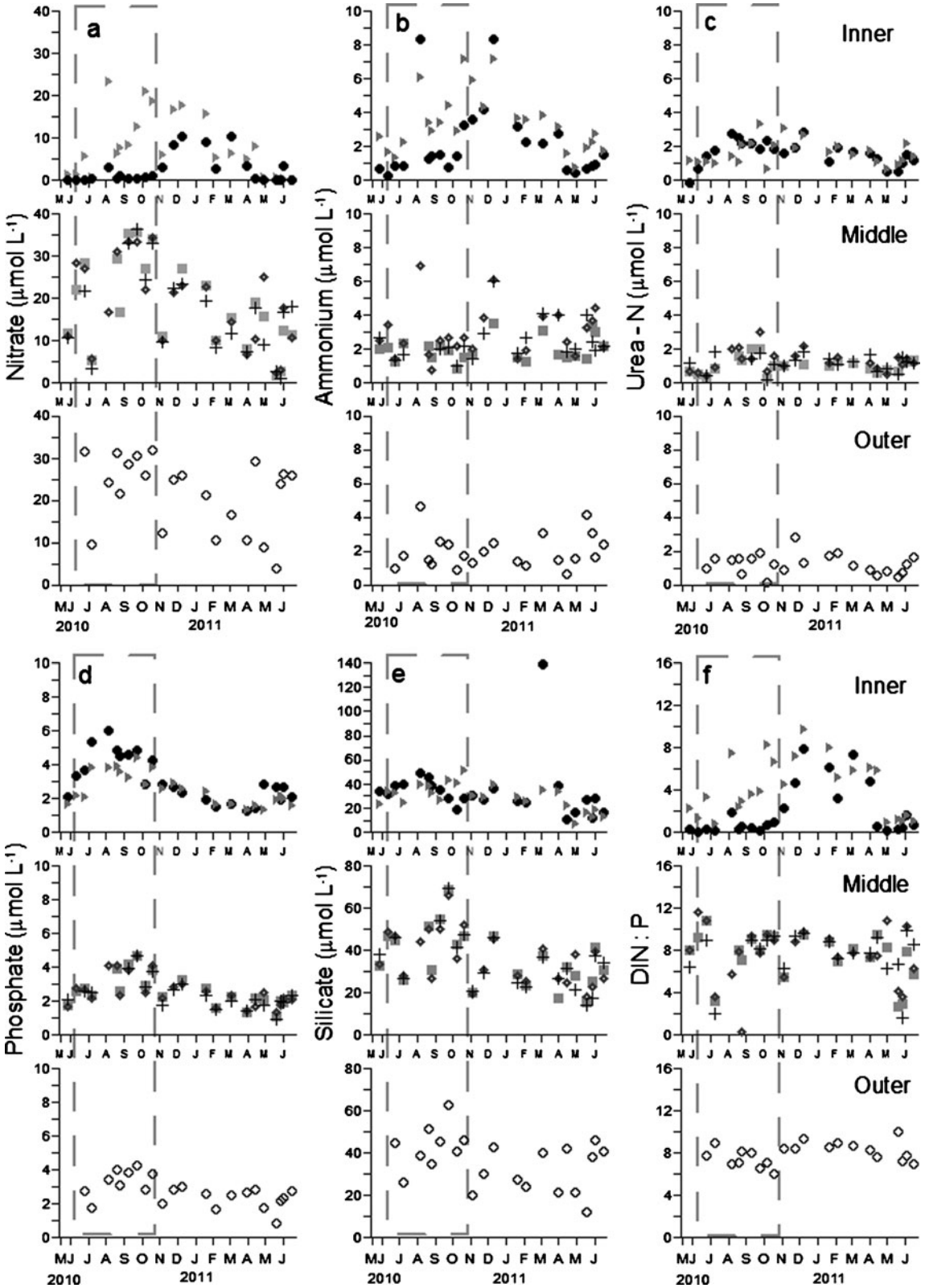

Fig. 4 Time series for nutrients **a** NO_3, **b** NH_4, **c** urea, **d** PO_4, **e** $Si(OH)_4$ and **f** DIN/P from May 2010 to June 2011. The inner Estero sites are indicated for DE1 (*filled circle*), DE2 (*filled triangle*); middle sites DE20 (*plus symbol*), DE13 (*empty diamond*), DE18 (*filled square*) and outer site DEM (*empty circle*). Note *y*-axis scale differences in silicate. The dry-upwelling season is indicated by the *dashed box*

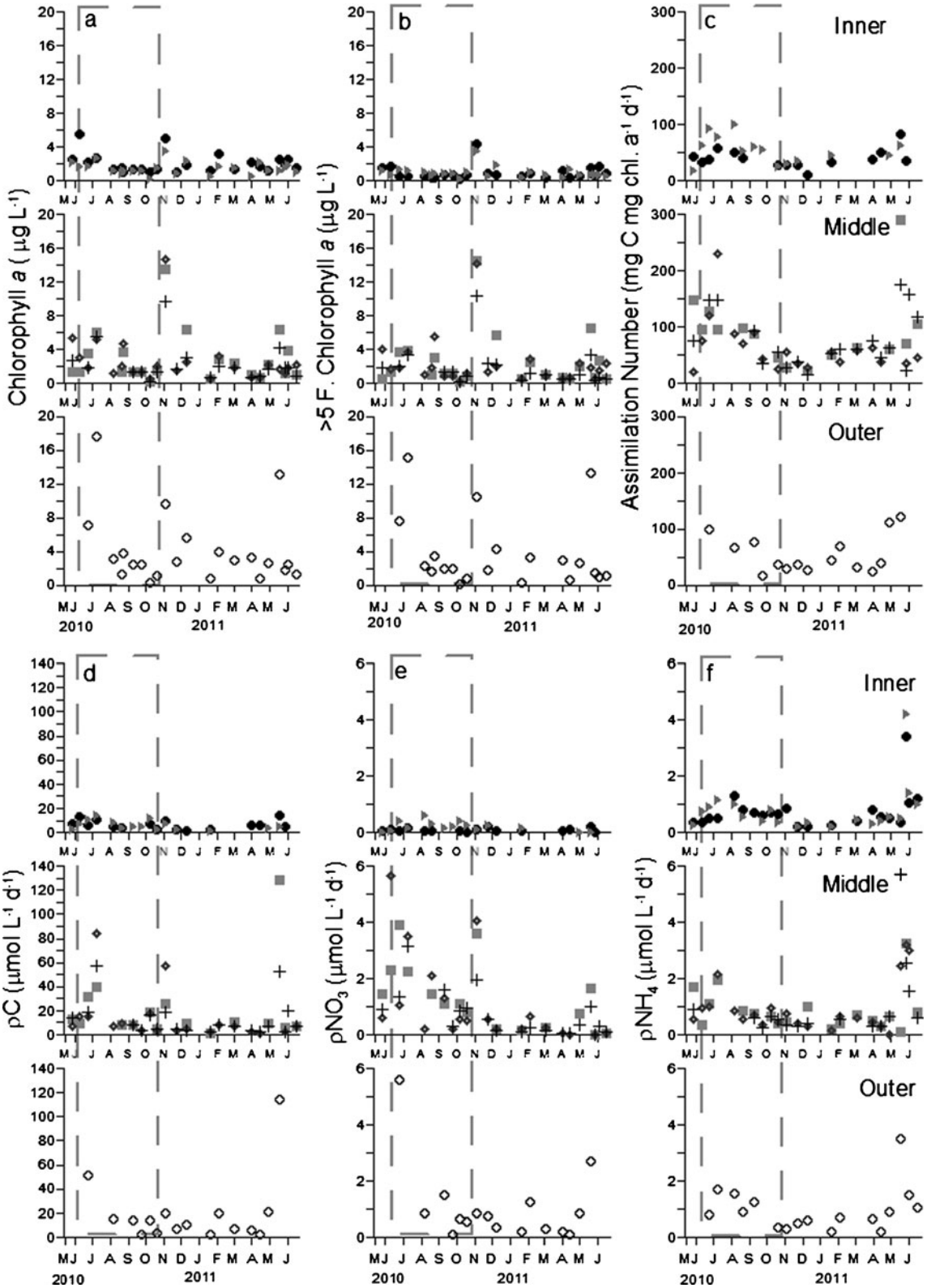

Fig. 5 Time series for **a** chlorophyll *a*, **b** >5-µm fraction chlorophyll *a*, **c** assimilation number, **d** ρC, **e** ρNO_3, and **f** ρNH_4 from May 2010 to June 2011. Inner sites are indicated for DE1 (*filled circle*), DE2 (*filled triangle*); middle sites DE20 (*plus symbol*), DE13 (*empty diamond*), DE18 (*filled square*) and outer site DEM (*empty square*). The dry-upwelling season is indicated by the *dashed box*

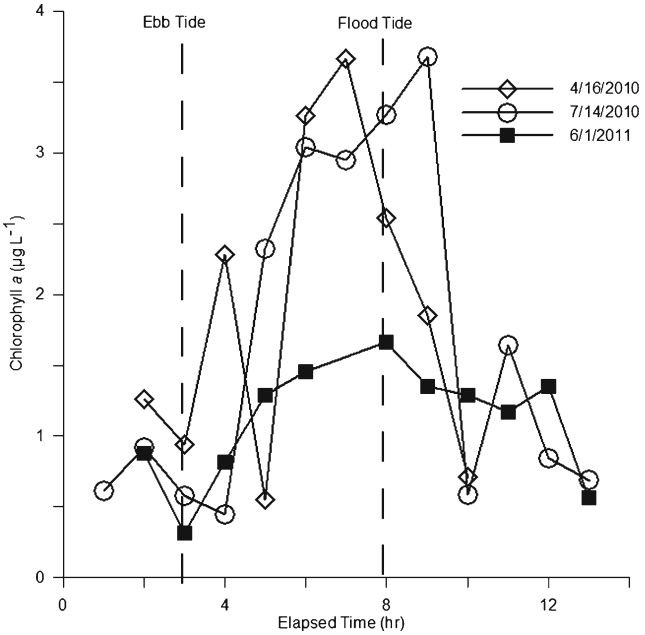

Fig. 6 Chlorophyll *a* concentrations at the outer site, DEM, measured hourly over three different tidal time series, each normalized to the time of the tidal cycle

Assimilation numbers were significantly greater at the outer and middle sites compared to the inner sites (ANOVA, $F(2,103)=5.59$, $p=0.0049$) (Fig. 5c) with the greatest values at the middle Estero. The maximum value were observed in spring 2011 at DE18 (289.2 mg C mg chl a^{-1} day^{-1}) (Fig. 5c) and the lowest at the inner Estero (DE1, 9.7 mg C mg chl a^{-1} day^{-1}) (Fig. 5c). The annual mean assimilation number at DEM, was similar to DE2; however, the maximum daily assimilation number at DEM (121.9 mg C mg chl a^{-1} day^{-1}) was higher (Table 1, Fig. 5c). The mean estimate of depth-integrated carbon uptake was 315 mg of C m^{-2} day^{-1} Estero-wide with the maximum value of 774 mg of C m^{-2} day^{-1} at DE18 and minimum at 119 mg of C m^{-2} day^{-1} at DE1.

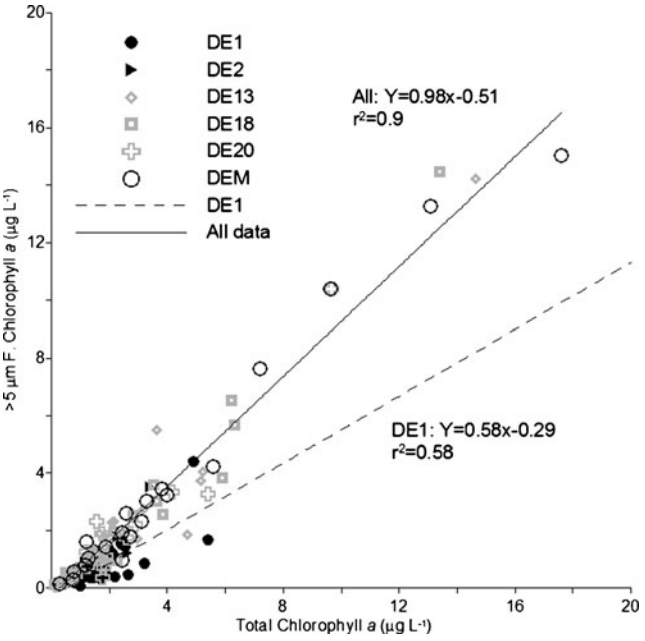

Fig. 7 Size fractioned chlorophyll *a* (in cells >5 µm diameter) plotted versus total chlorophyll *a* (all cells captured by GF/F). Inner sites are indicated for DE1 (*filled circle*), DE2 (*filled triangle*); middle sites DE20 (*open grey plus signs*), DE13 (*open grey diamonds*), DE18 (*open grey squares*) and outer site DEM (*empty circle*). All data linear fit regression is indicate by a solid line. DE1 linear fit regression is *grey dashed line*

Nitrogen Uptake and *f*-ratio

Nitrate uptake rates (ρNO_3) were generally greater than ρNH_4 at the three most coastal sites (DEM, DE18 and DE13; Table 1, Fig. 5e, f) but not significantly different (ANOVA, $F(1,108)=1.12$, $p=0.292$). In contrast, the annual mean ρNH_4 was significantly greater than ρNO_3 at the inner and more landward middle sites (DE20, DE2, and DE1) (ANOVA, $F(1, 105)=8.85$, $p=0.004$) (Table 1). The greatest mean ρNO_3 was measured at DE18 (Fig. 5e), while the highest values of ρNO_3 were at DEM (5.62 µmol l^{-1} day^{-1}) and DE13 (5.65 µmol l^{-1} day^{-1}) (Fig. 5e). The mean ρNO_3 for the dry-upwelling season (Table 2) was greater than the annual mean at all of the sites (Table 1). Ammonium uptake rates (ρNH_4) were low throughout the study period except for May 2011 when an increase was observed at all sites (Fig. 5f). Ammonium uptake rates (ρNH_4) were not significantly higher at the outer and middle Estero than the inner Estero (ANOVA, $F(2,113)=0.55$, $p=0.578$) (Fig. 5f). The maximum ρNH_4 was observed at DE20 (max=5.73 µmol l^{-1} day^{-1}; Fig. 5f).

The specific uptake rate (V) is the N taken up by the algae on a particulate N basis (Dugdale and Wilkerson 1986) This biomass specific parameter gives more a measure of the physiological uptake compared to ρ, the transport rate of nutrient per liter of sea water. VNO_3 followed spatial patterns similar to ρNO_3 with highest rates at the middle Estero, and the maximum rate at DE13 (2.2 day^{-1}) (Fig. 8a). VNO_3 was significantly greater at the middle and outer Estero compared to the inner Estero (ANOVA, $F(2, 100)=5.68$, $p=0.0046$). VNH_4 was similar by region (ANOVA, $F(2,113)=0.323$, $p=0.725$) with the greatest VNH_4 measured at DE2 (max=3.8 day^{-1}) (Fig. 8b).

The *f*-ratios were >0.5 at the outer and middle Estero from May to November 2010, corresponding to the dry-upwelling season with the highest ambient NO_3 and lowest NH_4 concentrations (Table 1, Fig. 9). In December 2010 following the start of the wet season the *f*-ratio decreased (Fig. 9). At DE1 and DE2, the *f*-ratio was <0.5 (Table 2, Fig. 9) throughout the entire study.

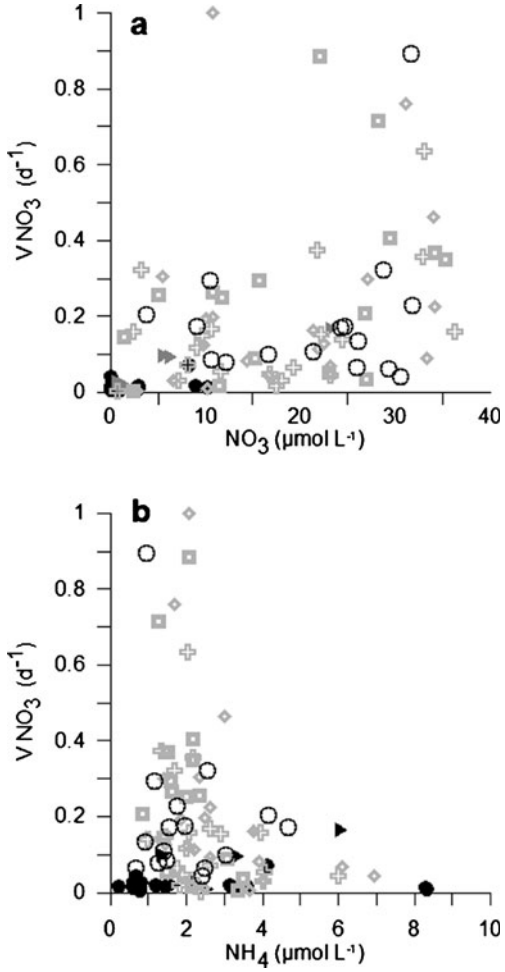

Fig. 8 Nitrate upake, VNO_3 versus **a** NO_3 concentration and **b** NH_4 concentration. Inner sites are indicated for DE1 (*filled circle*), DE2 (*filled triangle*); middle sites DE20 (*open grey plus signs*), DE13 (*open grey diamonds*), DE18 (*open grey squares*) and outer site DEM (*empty circle*). Note that the axes are on different scales

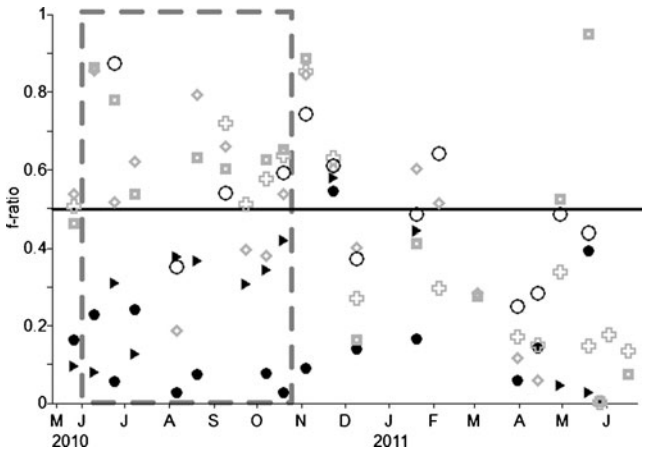

Fig. 9 The *f*-ratio in Drakes Estero from May 2010 to June 2011. Inner sites are indicated for DE1 (*filled circle*), DE2 (*filled triangle*); middle sites DE20 (*open grey plus signs*), DE13 (*open grey diamonds*), DE18 (*open grey squares*) and outer site DEM (*empty circle*). The 50 % line is indicated by a *horizontal solid line*. The dry-upwelling season is indicated by the *dashed box*

Phytoplankton species composition

Phytoplankton communities observed in this study were dominated by algal functional groups containing larger cells (i.e., dinoflagellates, centric and pennate diatoms) in the outer and middle Estero, while smaller size cells (flagellate algae [2–200 μm], dominated in the inner Estero (Fig. 10). Centric diatoms comprised 65 % to 80 % of the phytoplankton community within the middle and outer Estero during the dry-upwelling season (Fig. 10). The diatoms were a mixture of species (e.g., *Asterionellopsis* sp. and *Chaetoceros* sp.) with no particular dominant chain-forming diatom. Diatom chains present were two to three cells long. Non chain-forming *Chaetoceros socialis* and *Thalassiosira* sp. were among the dominant species within the centric diatoms. At DE1 small flagellates (2–200 μm), represented >79 % of the phytoplankton community during all dates and there was a higher proportion of dinoflagellates during the fall (Fig. 10). During the fall bloom at DE13 and DEM (Fig. 5a) dinoflagellates represented >60 % of total cells (Fig. 10), with *Prorocentrum micans* as the dominant species. The greatest concentrations

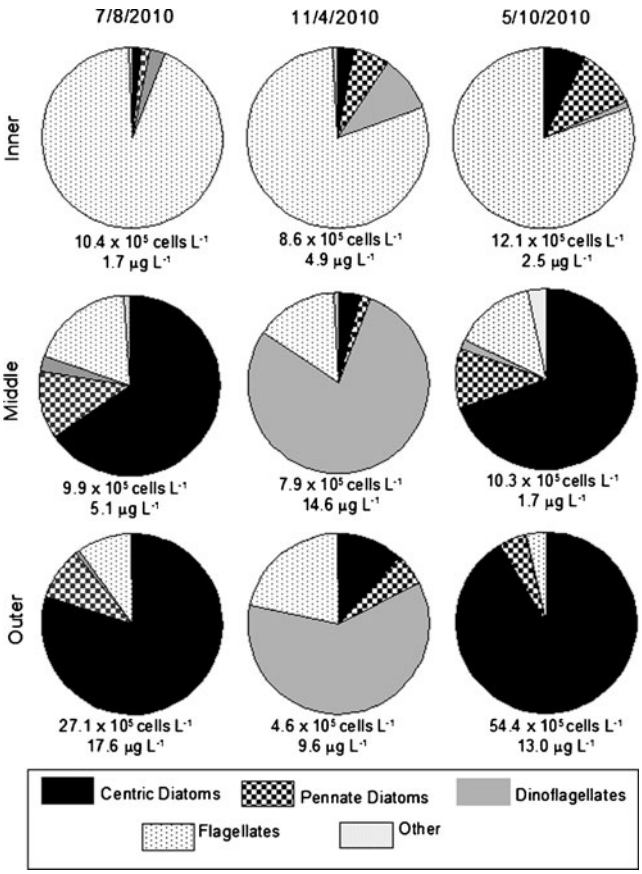

Fig. 10 Proportion of community composition of phytoplankton functional groups making up the community for inner (DE1), middle (DE13), and outer (DEM) sites of Drakes Estero. The total concentration of phytoplankton cells and the total chlorophyll *a* for each sample are displayed below chart

of phytoplankton cells were observed at DEM when there was the greatest chlorophyll *a* concentration on 8 July 2010 and 10 May 2010 (Fig. 10). The chlorophyll *a* concentrations were lowest at DE1, but the total concentrations of phytoplankton cells were greater than DE13 for all enumerated dates and DEM in the fall (4 Nov. 2010) (Fig. 10). The high concentrations of enumerated phytoplankton at DE1 were due to a high number of small flagellates (Fig. 10).

Discussion

Drakes Estero is strongly influenced by imported salty cold upwelled water. A conceptual model for the dry-upwelling season to illustrate the patterns in phytoplankton, DIN concentrations and phytoplankton N use is shown in Fig. 11, with a gradient from outer to inner Estero. In the outer Estero, associated with the cold ocean water, there are high concentrations of chlorophyll *a*, dominated by larger phytoplankton including centric diatoms. The major form of DIN is NO_3 and that is used by the phytoplankton for N productivity resulting in a high *f*-ratio. A similar set of conditions occurs in the middle Estero to a lesser degree with less chlorophyll *a* (again dominated by larger cells and diatoms), lower DIN, but still primarily NO_3 and NO_3 uptake by the phytoplankton with *f*-ratios greater than 0.5. Finally, in the inner Estero the influence of the upwelled water is diminished such that chlorophyll *a* is low, dominated by smaller cells and mostly small flagellates. The DIN concentration is low but dominated by NH_4 that is used by the phytoplankton resulting in a low *f*-ratio, below 0.5.

Spatial nutrient patterns in Drakes Estero are different from estuaries with minimal anthropogenic disturbances on the U.S. East Coast, such as Apalachicola Bay in the Gulf of Mexico where the productivity and mariculture facilities are fueled by riverine and not oceanic input (Mortazavi et al. 2000; Oczkowski et al. 2011). The prolonged periods of decreased precipitation and increased upwelling index during the dry-upwelling season (June to November; Figs. 2 and 3) creates spatial nutrient gradients in the Estero due to the import of ocean nutrients via tidal mixing and lack of land-based riverine nutrient input. The dependence on coastal nitrogen sources versus little to no terrestrial N input is a unique property of Drakes Estero compared to many other estuarine systems studied along the U.S. West Coast. For example, Elkhorn Slough adjacent to Monterey Bay, California, experiences high anthropogenic terrestrial nutrient loading during the wet season (Caffrey et al. 2002) and in Yaquina Bay, OR where anthropogenic inputs are minimal, although upwelled nutrients dominate in the dry season, land based nutrients dominate in the wet season (Brown and Ozretich 2009).

Drakes Estero shows high spikes in chlorophyll *a*, primary productivity, ρNO_3 and ρNH_4 (Fig. 5). These high values influence the annual and seasonal averages and increase the standard deviations (Tables 1 and 2) and standard errors. Daily variability was not addressed within the Estero but the data collected focused on conditions during flood tide. The increase in chlorophyll *a* observed during flood tide at the outer Estero location (Fig. 6) indicates that there is variability of the conditions during the day due to tidal influence within at least the outer Estero where mixing with oceanic water is greatest. The oceanic conditions are likely the cause of the high variability causing episodic periods of greater phytoplankton biomass and nutrient uptake. Relationships between the influence of oceanic conditions due to wind stress and estuarine conditions have been described within eastern boundary systems (Roegner et al. 2002; Brown and Ozretich 2009).

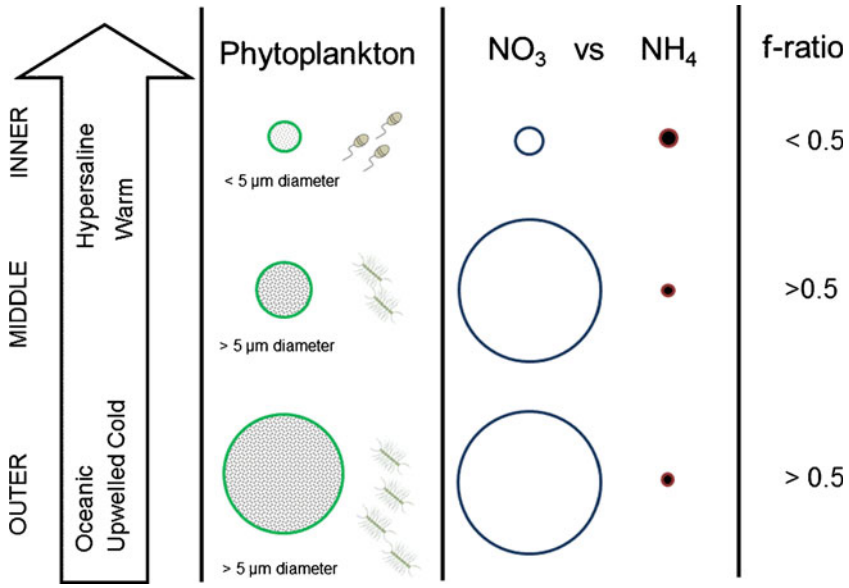

Fig. 11 Conceptual model of the phytoplankton, nitrogen concentrations and *f*-ratio during the dry-upwelling season in the outer, middle and inner Drakes Estero. This diagram highlights the spatial changes on the sea-to-land axis and the importance of imported upwelled nitrate to the outer and middle Estero fueling new primary productivity and imported chlorophyll *a*. The size of the symbol represents quantity of phytoplankton or nutrient

The ~50 % decline in chlorophyll *a* from the coastal (DEM) site landward (DE1) (Table 1) is similar to some other estuaries on the U.S. West Coast such as Willapa Bay, WA where there is an adjacent upwelled nutrient source supplying the ecosystem (e.g., Newton and Horner 2003), but different from Tomales Bay, California, a LIE in close proximity to Drakes Estero, where the chlorophyll *a* maximum is in the middle region (Kimbro et al. 2009). The chlorophyll *a* pattern in Drakes Estero is likely influenced by the shift in cell size of chlorophyll *a* containing cells with essentially all of the chlorophyll *a* in larger cells (i.e., >5-μm cells) at the outer and middle Estero compared to the majority of chlorophyll *a* in smaller cells (<5 μm) at the inner Estero (Table 1, Fig. 7).

The inner Estero had lower chlorophyll *a* concentrations, but a higher concentration of cells dominated by small flagellates than the middle Estero (Fig. 10). This study did not account for the picophytoplankton and picocyanobacteria (<2 μm) that have low chlorophyll *a* concentrations and are potentially important to primary productivity. The <2 μm fraction of phytoplankton can be important to primary productivity in the global oceans (Glover et al. 1986; Li 1994). A study off the coast of South Island, New Zealand, a nutrient-rich upwelling region, found that <2 μm fraction contributed substantially (>80 % particulate N and 39 % to 55 % of total chlorophyll *a*) to phytoplankton biomass (Hall and Vincent 1990). The small fraction may contribute to the food web of Drakes Estero, especially in the inner hypersaline reaches during the dry-upwelling season where NO_3 is depleted. Studies of some cyanobacteria (e.g., *Prochlorococcus*) have shown that it grows well on NH_4 and cannot utilize NO_3 (Moore et al. 2002). Decreasing species richness of picophytoplankton have been observed along an increasing salinity gradient within a hypersaline estuary (Shapira et al. 2010).

The elevated chlorophyll *a* concentrations in the outer and middle Estero (Fig. 5a) and the increase in chlorophyll *a* on flood tides (Fig. 6) indicate an import of phytoplankton along with nutrients, from coastal waters into the Estero. The import of chlorophyll *a* and oceanic phytoplankton taxa has been observed in other estuaries along the west coast of the USA (Newton and Horner 2003; Banas et al. 2007; Roegner and Shanks 2001). Dominance by larger phytoplankton cells and a 1:1 relationship between chlorophyll *a* in cells >5 μm and total chlorophyll *a* is characteristic of upwelling areas, e.g., in California (Wilkerson et al. 2000, 2006b). The coastal diatom species present in the Bodega Bay, California upwelling plume (Lassiter et al. 2006) and other California upwelling regions such as Monterey Bay (Wilkerson et al. 2000, 2006b) were observed in this study in Drakes Estero, including the diatoms *Chaetoceros socialis* and *Thalassiosira* sp.

An alternative explanation for the declining pattern in chlorophyll *a* from the outer to inner Estero (Figs. 5a and 6) may be the consumption of phytoplankton by grazers including farmed oysters (*C. gigas*) as well as native bivalve species (i.e., *Clinocardium nuttallii*, *Gemma gemma*, *Nutricola confuse*, and *Musculista senhousia*). In Willapa Bay, Washington, Banas et al. (2007) modeled different grazing rates and found that oysters and other bivalves were consuming phytoplankton and suggested this may be a reason for low phytoplankton biomass, with 8–15 % of the net supply lost to consumers. In addition to grazing, the elevated water temperature of the inner Estero (Fig. 3) may also influence phytoplankton community structure since diatoms are favored in cold water (Lomas and Glibert 1999) and so are less likely to be abundant in the warmer landward Estero.

Nitrate and NH_4 concentrations influenced phytoplankton N uptake. For example, throughout the entire study at DE1 where NO_3 was typically <0.5 μmol l^{-1}, VNO_3 was low, whereas at DEM, NO_3 was always >3.8 μmol l^{-1} and the measured VNO_3 was much higher (Table 1, Fig. 8a). However, these relationships are complicated through the interaction between NH_4 and NO_3 (Dortch 1990). Specifically, NH_4 can inhibit NO_3 uptake or prevent access by phytoplankton to the NO_3 pool (e.g., Wilkerson et al. 2006a; Dugdale et al. 2007; Parker et al. 2012). Dugdale et al. (2007) suggested for the nearby San Francisco Estuary, that NH_4 >4 μmol l^{-1} negatively impacted phytoplankton NO_3 uptake in the diatom-dominated phytoplankton community, and concentrations as low as 1 μmol l^{-1} NH_4 were reported to decrease NO_3 uptake in Piraeus Harbor water (Packard et al. 1971). In Drakes Bay, elevated NH_4 concentrations delayed NO_3 uptake (Dugdale et al. 2006), and after the NH_4 was drawn down below inhibitory levels there was a diatom bloom that depleted the upwelled NO_3 source in 3 to 7 days (Wilkerson et al. 2006b). Similar interactions appeared to be occurring in Drakes Estero where the highest VNO_3 values were observed when NH_4 was about <4 μmol l^{-1} (Fig. 8b). When the NH_4 concentrations were >4 μmol l^{-1} (Fig. 4b) on 6 August 2011 there were the lowest ρNO_3 values (Fig. 5e) observed during the dry-upwelling season at the outer and middle Estero.

There are two observed regions in Drakes Estero based upon the form of nitrogen being supplied (oceanic and inner) during the dry-upwelling season. The "oceanic" region encompasses the outer and middle Estero where there is "new" upwelled sourced NO_3 imported from oceanic sources. The "inner" region is where the N source is "regenerated" NH_4. However, during the transitional and winter seasons when precipitation increases, the *f*-ratios decrease, and the source of "new" and "regenerated" nitrogen to the Estero is more difficult to distinguish since then landward sources of N, such as NH_4 or urea may be supplying new N to the system (Fig. 9). New production dominated in the outer Estero (Fig. 9), with *f*-ratios similar to the Bodega upwelling plume to the north (0.4–0.8; Dugdale et al. 2006). Lower *f*-ratios have been observed in other inshore bays and estuaries adjacent to upwelling coasts, such as Saldahna Bay in South Africa where productivity is dominated by regenerated production and *f*-ratio is similar to the adjacent southern Benguela upwelling

coast (~0.2; Probyn 1992; Monteiro et al. 1998). In riverine dominated estuarine systems, i.e., Apalachacola Bay, the *f*-ratio is higher during the winter, due to NO_3 supply from elevated precipitation that is brought in by riverine input (Mortazavi et al. 2000). This did not seem to be the case in Drakes Estero (Figs. 2, 4 and 9).

There was a shift in phytoplankton communities from diatoms in the spring and dry-upwelling season to dinoflagellates in the fall that follows Margalef's Mandala (Margalef 1978) of temperate blooms during the cold turbulent spring and the calm fall containing different functional groups (1978). After the first rainfall during fall 2010, there was a bloom of the dinoflagellate *Prorocentrum micans* (Fig. 2a). This species is sometimes considered a nuisance species (Horner et al. 1997; Glibert et al. 2012). *P. micans* is a mixotrophic dinoflagellate (Jeong et al. 2005) that can carry out heterotrophic feeding in addition to photosynthesis. It is possible that mixotrophy contributed to the N nutrition of the *P. micans* bloom, because lower N (NO_3 and NH_4) uptake rates were measured than would be predicted based on the C uptake rates that were associated with the bloom (Fig. 5). Blooms of *P. micans* have also been observed in highly stratified and nutrient depleted southern California coastal waters (Shipe et al. 2008).

Published estimates of phytoplankton productivity and nutrient uptake in small and shallow estuaries and bays, especially LIEs, are rare in comparison to larger estuaries and coastal upwelling regions. Estimates of daily depth integrated primary production for Drakes Estero (mean 315 mg C m^{-2} day^{-1}) are low compared to other estuaries influenced by upwelled nutrient sources such as Willapa Bay (median=3,000 mg C m^{-2} day^{-1}; Newton and Horner 2003) and Saldahna Bay, South Africa (mean=3,400 mg C m^{-2} day^{-1}; Pitcher and Calder 1998). However, primary production is higher in Drakes Estero compared to nearby San Francisco Estuary, a highly urbanized estuary with low chlorophyll biomass (maximum=114 mg C m^{-2} day^{-1}; Kimmerer et al. 2012). The shallow depth in Drakes Estero limits the volume of the water column that phytoplankton productivity can occur and this may contribute to lower depth-integrated values.

Nutrient uptake rates in Drakes Estero (Table 1, Fig. 5) are similar to the California region (e.g., Dugdale et al. 2006). Despite the lower depth integrated water column C uptake than in other estuaries, DIN uptake rates (especially the biomass-specific rates) in the Estero indicate that the phytoplankton are growing rapidly. DIN uptake rates are higher in the Estero (annual maximum mean $V NO_3$=0.27 day^{-1}, $V NH_4$=0.33 day^{-1}) (Table 1, Fig. 5), than in Central San Francisco Bay, a light-limited system with elevated NH_4 (spring mean $V NO_3$ of 0.08 day^{-1} and $V NH_4$ of 0.15 day^{-1}) (Wilkerson et al. 2006a). In the nearby Bodega Bay upwelling plume the maximum new production rate (maximum ρNO_3= 4.3 μmol l^{-1} day^{-1}) was less than measured maximum rate in the outer and middle Drakes Estero (5.7 μmol l^{-1} day^{-1}; Fig. 5e), and the $V NO_3$ values in the Bodega plume (maximum=~1.2 day^{-1}; Dugdale et al. 2006) were lower (by ~50 %) than in Drakes Estero (2.2 day^{-1}). Likely, these elevated $V NO_3$ values in the outer and middle Estero reflect a physiologically well adapted phytoplankton population (i.e., shifted up) as defined by Dugdale et al. (1990) when rates of $V NO_3$ exceed 0.24 day^{-1} (0.03 h^{-1}) and the phytoplankton were responding to upwelled NO_3 entering into Drakes Estero.

In addition to providing baseline data for this LIE for nutrients, phytoplankton and nutrient uptake, increasing our knowledge of phytoplankton dynamics is essential for Drakes Estero which may soon be undergoing substantial change with the removal of the mariculture facility including the large quantity of farmed oysters that have been there for the last 80 years. Such information will provide insight to the influence of oyster mariculture on nutrient concentrations and phytoplankton biomass within LIEs. If the aquaculture facility is removed the Estero may show a decrease in regenerated NH_4 concentrations, an increase in chlorophyll *a*, and a shift in phytoplankton community structure to larger phytoplankton functional groups (diatoms and dinoflagellates) in the regions with longer residence times. Studies, such as this one, that relate the influence of coastally upwelled nutrients in shallow pristine estuaries to primary production are valuable for management decisions and for comparison to estuaries where anthropogenic nutrients are causing adverse impacts to ecosystems.

Acknowledgments Research and academic experiences were funded in part by the PADI Foundation, Achievement Rewards for College Scientists, California State Universities (CSU) Council on Ocean Affairs, Science & Technology (COAST), College of Science and Engineering and Department of Biology at SFSU, a CSU Pre-Doctoral Scholarship, and the Sally Cassanova Scholarship. A thank you for assisting with the laboratory, field, or logistics of this project goes to J. Largier, A. Marchi, Drakes Bay Oyster Company, B. Becker of the National Park Service; the RTC community, E. Carpenter, S. Blaser, E. Kress, J. Fuller, A. Johnson, J. Lee, J. Huggans, M. Maheigan and A. Pimenta.

References

Arar, E.J. and G.B. Collins.1992. In vitro determination of chlorophyll a and pheophytin a in marine and freshwater phytoplankton by fluorescence. In: Methods for the Determination of Chemical Substances in Marine and Estuarine Environmental Samples. Report # EPA/600/R-92/121. Cincinnati, OH: Environmental Monitoring and Support Laboratory, Office of Research and Development, U.S. Environmental Protection Agency.

Bakun, A. 1973. Coastal upwelling indices, west coast of North America, 1946–1971. U.S. Department of Commerce, NOAA technical report, NMFS SSRF-671.

Banas, N.S., B.M. Hickey, J.A. Newton, and J.L. Ruesink. 2007. Tidal exchange, bivalve grazing, and patterns of primary production in Willapa Bay, Washington, USA. *Marine Ecology Progress Series* 341: 123–139.

Bran and Luebbe Inc. 1999a. *Silicate in water and seawater. AutoAnalyzer Method No. G-177-96*. Buffalo Grove, IL: Bran and Luebbe, Inc.

Bran and Luebbe Inc. 1999b. *Bran Luebbe AutoAnalyzer Applications: AutoAnalyzer Method No. G-175-96 phosphate in water and seawater*. Buffalo Grove, IL: Bran and Luebbe Inc.

Bran and Luebbe Inc. 1999c. *Bran Luebbe AutoAnalyzer Applications: AutoAnalyzer Method No. G-172-96 nitrate and nitrite in water and seawater*. Buffalo Grove, IL: Bran and Luebbe Inc.

Brown, C.A., and R.J. Ozretich. 2009. Coupling between the coastal ocean and Yaquina Bay, Oregon: Importance of oceanic inputs relative to other nitrogen sources. *Estuaries and Coasts* 32: 219–237.

Caffrey, J.M., N. Harrington, and B. Ward. 2002. Biogeochemical processes in a small California estuary: 1. Benthic fluxes and pore water constituents reflect high nutrient freshwater inputs. *Marine Ecology Progress Series* 233: 39–53.

California Department of Public Health. 2010. 2010 Management Plan for Commercial Shellfishing in Drakes Estero. Technical Report 10–05.

Dortch, Q. 1990. The interaction between ammonium and nitrate uptake in phytoplankton. *Marine Biology* 331: 221–232.

Dugdale, R.C., and J.J. Goering. 1967. Uptake of new and regenerated forms of nitrogen in primary productivity. *Limnology and Oceanography* 12: 196–207.

Dugdale, R.C., and F.P. Wilkerson. 1986. The use of ^{15}N to measure nitrogen uptake in eutrophic oceans: Experimental considerations. *Limnology and Oceanography* 31: 673–689.

Dugdale, R.C., F.P. Wilkerson, and A. Morel. 1990. Realization of new production in coastal upwelling areas: A means to compare relative performance. *Limnology and Oceanography* 35(4): 822–829.

Dugdale, R.C., F.P. Wilkerson, V. Hogue, and A. Marchi. 2006. Nutrient controls on new production in the Bodega Bay, California, coastal upwelling plume. *Deep Sea Research* 53: 3049–3062.

Dugdale, R.C., F.P. Wilkerson, V.E. Hogue, and A. Marchi. 2007. Spring phytoplankton bloom development in San Francisco Estuary: the role of ammonium and nitrate. *Estuarine, Coastal and Shelf Science* 73: 17–29.

Dumbauld, B.R., J.L. Ruesink, and S.S. Rumbrill. 2009. The ecological role of bivalve shellfish aquaculture in the estuarine environment: A review with application to oyster and clam culture in West Coast (USA) estuaries. *Aquaculture* 290: 196–223.

Figueiras, F.G., U. Larbarta, and M.J. Fernandez Reiriz. 2002. Coastal upwelling, primary production and mussel growth in the Rias Baixas of Galicia. *Hydrobiologia* 484: 121–131.

Glibert, P.M., J.M. Burkholder, and T.M. Kana. 2012. Recent insights about relationships between nutrient availability, forms, and stoichiometry, and the distribution, ecophysiology, and food web effects of pelagic and benthic *Prorocentrum* species. *Harmful Algae* 14: 231–259.

Glover, H.E., D.A. Bhinney, and C.S. Yentsch. 1986. Photosynthetic characteristics of picoplankton compared with those of larger phytoplankton populations in various water masses in the gulf of Maine. *Biological Oceanography* 3: 223–248.

Hall, J.A., and W.F. Vincent. 1990. Vertical and horizontal structure in the picophytoplankton communities of a coastal upwelling system. *Marine Biology* 106(3): 465–471.

Hickey, B.M. 1989. Patterns and processes of circulation over the Washington continental shelf and slope. *Oceanography* 47: 41–115.

Hickey, B., and N. Banas. 2003. Oceanography of the U.S. Pacific Northwest coastal ocean and estuaries with application to coastal ecology. *Estuaries and Coasts* 26: 1010–1031.

Horner, R.A., D.L. Garrison, and F.G. Plumley. 1997. Harmful algal blooms and red tide problems on the US west coast. *Limnology and Oceanography* 42: 1076–1088.

Jeong, H.J., J.Y. Park, J. Nho, M.O. Park, J.H. Ha, K.A. Seong, C. Jeng, C.N. Seong, K.Y. Lee, and W.H. Yih. 2005. Feeding by red-tide dinoflagellates on the cyanobacterium *Synechococcus*. *Aquatic Microbial Ecology* 41: 131–143.

Kimbro, D., J. Largier, and E. Grosholz. 2009. Coastal oceanographic processes influence the growth and size of a key estuarine species, the Olympia oyster. *Limnology and Oceanography* 54: 1425–1437.

Kimmerer, W.J., A.E. Parker, U.E. Lidström, and E.J. Carpenter. 2012. Short-term interannual variability in primary production in the low-salinity zone of the San Francisco Estuary. *Estuaries and Coasts* 25: 913–929.

Largier, J. 2004. The importance of retention zones in the dispersal of larvae. *American Fisheries Society Symposium* 42: 105–122.

Largier, J. 2010. Low-Inflow estuaries: hypersaline, inverse and thermal scenarios. In Contemporary Issues in Estuarine Physics, ed. A. Valle-Levinson, A., 247–272. Cambridge University Press.

Largier, J.L., S.V. Smith, and J.T. Hollibaugh. 1997. Seasonally hypersaline estuaries in Mediterranean climate regions. *Estuarine, Coastal and Shelf Science* 45: 789–797.

Lassiter, A.M., F.P. Wilkerson, R.C. Dugdale, and V.E. Hogue. 2006. Phytoplankton assemblages in the CoOP-WEST coastal upwelling area. *Deep-Sea Research* 53: 3063–3077.

Legendre, L., and M. Gosselin. 1996. Estimation of N or C uptake rates by phytoplankton using ^{15}N or ^{13}C: Revisiting the usual computation formulae. *Journal of Plankton Research* 19: 263–271.

Li, William K.W. 1994. Primary production of prochlorophytes, cyanobacteria, and eukaryotic ultraphytoplankton: Measurements from a flow cytometric sorting. *Limnology and Oceanography* 39(1): 169–175.

Lomas, M.W., and P.M. Glibert. 1999. Interaction between ambient NH_4 and NO_3uptake and assimilation: Comparison of diatoms and dinoflagellates at several growth temperature. *Marine Biology* 133: 541–555.

Lund, J.W., G.C. Kipling, and E.D. Le Cren. 1958. The inverted microscope method of estimating algal numbers and the statistical basis of estimations by counting. *Hydrobiologia* 11: 143–170.

MacDonald, R.W., F.A. McLaughlin, and C.S. Wong. 1986. The storage of reactive silicate samples by freezing. *Limnology and Oceanography* 31: 1139–1142.

Margalef, R. 1978. Life-forms of phytoplankton as survival alternatives in an unstable environment. *Oceanologica Acta* 134: 493–509.

Monteiro, P.M.S., B. Spolander, G.B. Brundt, and G. Nelson. 1998. Shellfish mariculture in the Benguela system: Estimates of nitrogen-driven new production in Saldahna Bay using two physical models. *Journal of Shellfish Research* 17: 3–13.

Montes-Hugo, M.A. 2007. Two decades of aquaculture has not altered the phytoplankton communities of a coastal lagoon influenced by coastal upwelling. *Hidrobiologica* 17: 213–224.

Moore, L.R., A.F. Post, G. Rocap, and S.W. Chistholm. 2002. Utilization of different nitrogen sources by the marine cyanobacteria *Prochlorococcus* and *Synechococcus*. *Limnology and Oceanography* 47(4): 989–996.

Mortazavi, B., R.L. Iverson, W. Huang, F.G. Lewis, and J.M. Caffrey. 2000. Nitrogen budget of Apalachicola Bay, a bar-built estuary in the northeastern Gulf of Mexico. *Marine Ecology Progress Series* 195: 1–14.

Newton, J.A., and R.A. Horner. 2003. Use of phytoplankton species indicators to track the origin of phytoplankton blooms in Willapa Bay, Washington. *Estuaries* 26: 1071–1078.

Oczkowski, A., F. Lewis, S. Nixon, H. Edmiston, R. Robinson, and J. Chanton. 2011. Fresh water inflow and oyster productivity in Apalachicola Bay, FL (USA). *Estuaries and Coasts* 34: 993–1005.

Packard, T., T.R. Blasco, J.J. MacIsaac, and R.C. Dugdale. 1971. Variations in nitrate reductase activity in marine phytoplankton. *Investigacion Pesquera* 35(1): 209–219.

Parker, A.E., V.E. Hogue, F.P. Wilkerson, and R.C. Dugdale. 2012. The effect of inorganic nitrogen speciation on primary production in the San Francisco Estuary. *Estuarine, Coastal and Shelf Science* 104–105: 91–101.

Pitcher, G.C., and D. Calder. 1998. Shellfish mariculture in the Benguela system: Phytoplankton and the availability of food for commercial mussel farms in Saldahna Bay, South Africa. *Journal of Shellfish Research* 17(1): 15–24.

Probyn, T.A. 1992. The inorganic nitrogen nutrition of phytoplankton in the southern Benguela: New phytoplankton, phytoplankton size and implications for pelagic food webs. *South African Journal of Marine Science* 12(1): 411–420.

Revilla, M., J. Alexander, and P.M. Glibert. 2005. Urea analysis in coastal waters: Comparison of enzymatic and direct methods. *Limnology and Oceanography: Methods* 3: 290–299.

Roegner, G.C., and A.L. Shanks. 2001. Import of coastally-derived chlorophyll a to South Slough, Oregon. *Estuaries* 24: 244–256.

Roegner, G.C., B. Hickey, J.A. Newton, A. Shanks, and D.A. Armstrong. 2002. Wind-induced plume and blume intrusions into Willapa Bay, Washington. *Limnology and Oceanography* 47(4): 1033–1042.

Ruesink, J.L., G.C. Roegner, B.R. Dumbauld, J.A. Newton, and D.A. Armstrong. 2003. Contributions of coastal and watershed energy sources to secondary production in a northeastern Pacific estuary. *Estuaries* 26: 1079–1093.

Shapira, M., M.J. Buscot, T. Pollet, S.C. Leterme, and L. Seuront. 2010. Distribution of picophytoplankton communities from brackish to hypersaline waters in a south Australian coastal lagoon. *Saline sytems* 6(2).

Shipe, R.F., A. Leinweber, and N. Gruber. 2008. Abiotic controls of potentially harmful algal blooms in Santa Monica Bay, California. *Continental Shelf Research* 28: 2584–2593.

Solórzano, L. 1969. Determination of ammonia in natural waters by phenol hypochlorite method. *Limnology and Oceanography* 14: 799–801.

Smith, S.V., and J.T. Hollibaugh. 1997. Annual cycle and interannual variability of ecosystem metabolism in a temperate climate embayment. *Ecological Monographs* 67(4): 509–533.

U.S. Department of the Interior. 2012. Secretary Salazar issues decision on Point Reyes National Seashore permit. DOI news release. http://www.doi.gov/news/pressreleases/secretary-salazar-issues-decision-on-point-reyes-national-seashore-permit.cfm#. Accessed 1 Dec. 2012.

Vander Woude, A.J., J.L. Largier, and R.M. Kudela. 2006. Nearshore retention of upwelled waters north and south of Point Reyes (northern California) — Patterns of surface temperature and chlorophyll observed in CoOP WEST. *Deep Sea Research, Part II* 53: 2985–2998.

Whitledge, T.E., S.C. Malloy, C.J. Patton, and C.D. Wirick. 1981. Automated nutrient analyses in seawater. Brookhaven Natl. Lab. Formal Rep. BNL 51398.

Wilkerson, F.P., R.C. Dugdale, F.P. Chavez, and R.M. Kudela. 2000. Biomass and productivity in Monterey Bay, CA: Contribution of the larger autotrophs. *Deep-Sea Research II* 47: 1003–1022.

Wilkerson, F.P., R.C. Dugdale, V.E. Hogue, and A. Marchi. 2006a. Phytoplankton blooms and nitrogen productivity in San Francisco estuary. *Estuaries and Coasts* 29: 401–416.

Wilkerson, F.P., A. Lassiter, R.C. Dugdale, A. Marchi, and V. Hogue. 2006b. The phytoplankton bloom response to wind events and upwelled nutrients during the CoOP WEST study. *Deep Sea Research, Part II* 53: 3023–3048.